

Kinetic Structure Change of the Oxidation of Carbon Monoxide on Differently Prepared Zinc Oxides

Boris Golman*, Atsushi KASAI**, Tohru KANNO** and Masayoshi KOBAYASHI**

(Received May 6, 1993)

Abstract

The fine kinetic structure of CO oxidation over zinc oxides, which were differently prepared from Kadox ZnO (K25-ZnO) and Kanto Chemical Co. ZnO (Kan-ZnO), has been compared in detail by using both the steady state and the transient response methods. The apparent reaction rate surface of K25-ZnO has been visualized in the form of three dimensional surface as a function of P_{CO} and P_{O_2} at 130-170°C, which gives both maximum and minimum points on the surface. In the case of Kan-ZnO, the rate simply shows the first order with respect to P_{CO} and the zero order with respect to P_{O_2} . This extraordinary difference in kinetic structure can be considered as a result of the difference of crystal surface of original ZnO.

1. INTRODUCTION

Recently Bolis, Fubini and Giamello¹⁾ have demonstrated that reaction activity of zinc oxide surface, such as the adsorption CO and H₂, strongly depends on form of the crystallites. Three polycrystalline ZnO samples have been studied: one obtained by ignition of zinc metal (Kadox) and the others obtained by decomposition of zinc carbonate (c-ZnO) and oxalate (o-ZnO). Kadox ZnO gives the higher surface reactivity rather than the others. The adsorption enthalpy of CO is evaluated to be 46 kJ/mol on the reduced surface of Kadox whereas 8 kJ/mol on c-ZnO. The authors explained difference in adsorption capacity by taking into consideration the presence of better defined crystallites with sharp edges on the Kadox ZnO.

Based on these results, it has been proposed that catalytic activity and kinetic structure of reaction may drastically be changed depending on preparation routes of ZnO samples. The aim of this paper is to compare the kinetic structure of CO oxidation over two differently prepared ZnO, one of which is from Kadox 25 New Jersey Zinc Co. (K25-ZnO) and the other from Kanto Chemical Co. (Kan-ZnO).

Carbon monoxide oxidation on zinc oxide has been used for the subject of a large number of reaction mechanism and kinetic studies²⁻⁴⁾ as a model reaction in heterogeneous catalysis. They have roughly been classified into two groups based on: (1) Langmuir-Hinshelwood (L-H) mechanism, concerning chemisorbed CO and oxygen and (2) Eley-Rideal (E-R) mechanism with reaction between gaseous CO (or weakly adsorbed CO) and adsorbed oxygen. Also the two reaction pathways mechanism (one is L-H and the other is E-R pathways) may be proposed^{4,5)}, because different active species are located on the surface

* Chemical Environmental Engineering.

** Department of Chemical System Engineering.

such as O (neutral) and O⁻⁶. Recently many works involving multi-pathway reactions have been reported⁷. When this idea is accepted, the overall region of the variations in reaction conditions such as gas composition and reaction temperatures may be subdivided into three different regions, each of which has an advantageous pathway: (1) L-H pathway, (2) E-R pathway and (3) mixed pathway.

Generally, it is not so easy to clarify simultaneously the detail of comprehensive complex kinetic structure. The transient response method (TRM)^{8,9} is a powerful tool to elucidate the mechanism of single pathway reaction. Let us apply TRM to the three regions and call this new method the patterned transient response method (PTRM). In the present study PTRM will be proved to be a useful tool for the analysis of multi-reaction pathways.

2. EXPERIMENTAL PROCEDURE

A schematic layout of the equipment used for transient response experiments is shown in Fig. 1. The gases employed were supplied by Takachiho Chemical Co. (all > 99.7 pure). Flowrates were controlled using Okura mass flow valves with an accuracy of $\pm 3\%$.

In the present study, three gas streams could be set up, each containing a mixture of CO/O₂/He and He of any desired composition. These were directed to two four way valves that have three inlet ports, one for each feed stream, and three outlet ports, two to two bypass lines and the other to the reactor. The pressure in the bypass lines was adjusted using a needle valve to ensure that the pressure in the three streams was equal. It has been shown that the switching of the four port valve gave a good approximation to a step change in feed composition.

The reactor used was a Pyrex glass tube in which a electrical conductivity cell was located at the end of catalyst bed. Step changes using He/N₂ mixture showed that the

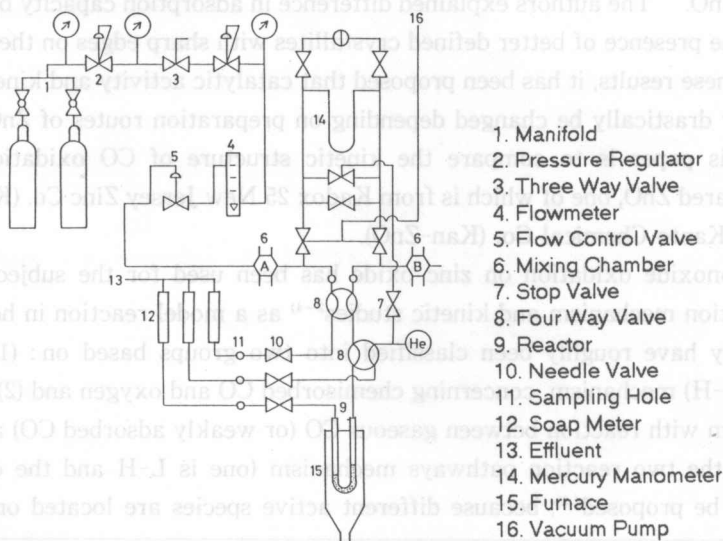


Fig. 1. Schematic layout of the experimental equipment used in the present study

reactor approximated very well to a piston flow reactor, in which the residence time was less than 15 sec.

The analysis was carried out using three Hitachi-164 chromatographs with a thermal conductivity detector. A Porapack Q column (1 or 2 m) was used for the analysis of CO₂ and a molecular sieve 5A column (0.5, 1 or 2m) was used to analyses CO, N₂ and O₂.

The catalysts used in this study are commercially available zinc oxide supplied from New Jersey Zinc Co. Kadox 25 and from Kanto Chemical Co. K25-ZnO was obtained from ZnCO₃ as a starting material, which is successively treated by the reduction, ignition, evaporation and oxidation in air, and Kan-ZnO was obtained from the oxidation of melted zinc metal. The X-ray diffraction analysis showed the same wurtzite-type crystalline structure of the two samples, whereas BET surface area was measured in a big difference as 4.0 m²/g for Kan-ZnO and 20 m²/g for K25-ZnO.

The electrical conductivity of the catalysts was measured by the same procedure as previously reported¹⁰. The catalyst (0.2 g) was sandwiched between two platinum electrode plates (0.97 mm i.d. and 0.5 mm thickness) pierced with 50 small holes. The d.c. conductivity was followed by measuring the voltage change of the standard resistor (100 σ) using a microvoltmeter (Ohkura AM-1001 A).

All experiments were carried out at 1 atm pressure and a total flowrate range of 100 - 200 cm³/min. Steady state experiments were performed to measure the effects of temperature, feed composition and space velocity on the activity of the catalysts. It has been shown by both experiment and calculation that under the experimental conditions chosen, both external and internal transport resistance are negligible.

NEC PC-9801DS was used to simulate the transient response curves. The reactor parameters used for the simulation are summarized in Table 1.

Table 1. List of Reactor Parameters

Catalyst	Reaction temperature	Catalyst surface area	Catalyst weight	Reactor length	Superficial gas velocity	Total amount of active sites		Porosity	Catalyst bed density
	(°C)					(m ² /g)	(g)		
	T	S	W	L	U	S _i	S _{ii}	ϵ	ρ_c
K25-ZnO	130 - 170	20	78.3 (20-40 mesh)	58.7	204	1.1	1.1	0.56	1.7
Kan-ZnO	190 - 250	4.0	189.6 (20-40 mesh)	154 (190-250°C) 55.4 (250°C)	221.3	1.6	2.7	0.56	1.7

3. RESULTS AND DISCUSSION

3-1. Adsorption of Oxygen

A previous study⁴⁾ showed that oxygen was adsorbed on the surface of Kan-ZnO to form both neutral and O^- species. The amounts of the two species were evaluated, from the O_2 - O_2 response curve and the O_2 - σ response curve, to be $0.8 \cdot 10^{-6}$ ($1.6 \cdot 10^{-6}$ mole/g for active sites) and $1.35 \cdot 10^{-6}$ ($2.7 \cdot 10^{-6}$ mole/g for active sites) mole O_2 /g, respectively⁴⁾. For K25-ZnO, by using the same techniques, they were given the same value $0.55 \cdot 10^{-6}$ mole O_2 /g ($1.1 \cdot 10^{-6}$ mole/g for active sites). The total amounts of the two active species were regarded as ones for the two active sites S_I and S_{II} . They were presented in Table 1.

3-2. Adsorption of CO and CO_2

The CO-CO response evaluated the amounts of adsorbed CO to be negligibly small on Kan-ZnO and $1.0 \cdot 10^{-6}$ mol/g on K25-ZnO without depending on the concentration of CO. Fig. 2 illustrates the change in the electrical conductivity of catalyst during the reaction at steady state on K25-ZnO as a function of P_{CO} , indicating no charge transfer between adsorbed CO and catalyst.

On the adsorption of CO_2 , it obeys a Langmuir isotherm with the saturated amount of $2.7 \cdot 10^{-6}$ mol/g on Kan-ZnO. A little amount of adsorption less than $3 \cdot 10^{-6}$ mol/g, on the other hand, is observed on K25-ZnO, and one may assume that the adsorbed CO_2 has no serious effect on the reaction rate at present reaction conditions.

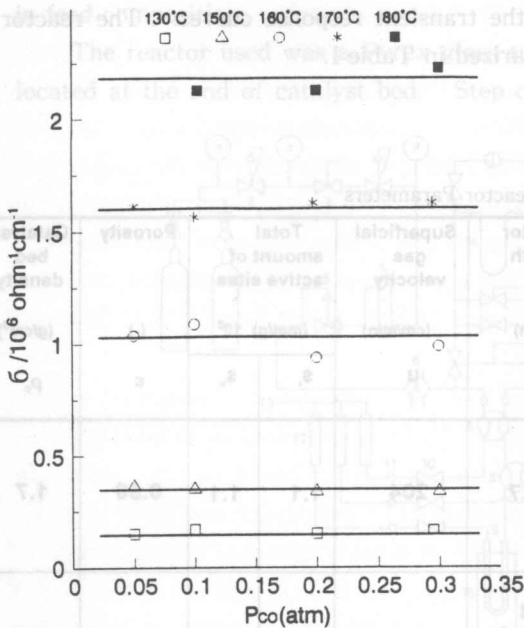


Fig. 2. Plots of σ as a function of P_{CO} on K25-ZnO; $P_{O_2} = 0.2$ atm.

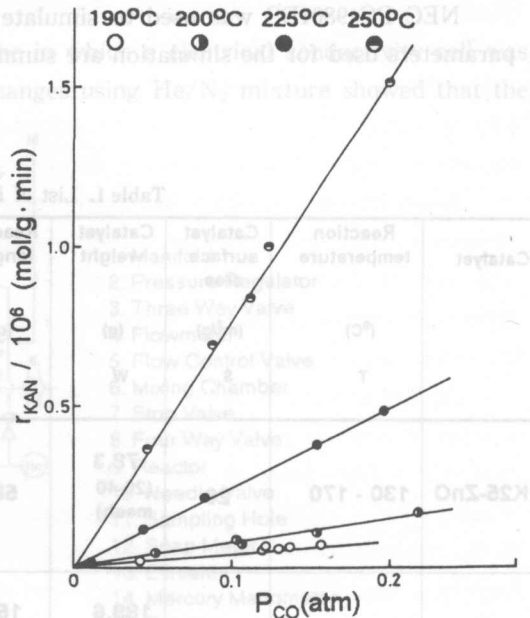


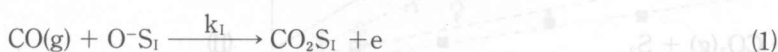
Fig. 3. Steady state rate r_{KAN} vs. P_{CO} on Kan-ZnO; $P_{O_2} = 0.2$ atm.

3-3. Reaction Model on Kan-ZnO

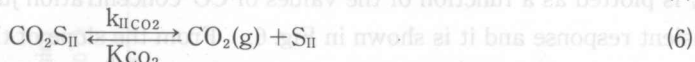
Fig. 3 illustrates the steady state rate as a function of P_{CO} . From this apparent linearity of the data, one can not recognize a two reaction pathway model. For the discrimination of the two pathway model, the transient response method can conveniently be applied.

The CO-CO₂ response curve indicated a characteristic mode which was derived into two parts: one was an instantaneous increase or decrease part at the initial stage of the response curve, and the other was a gradual change part approaching to a steady state level⁴⁾. To explain this mode, the two path reaction model was proposed as follows.

Reaction path I which corresponds to the instantaneous response part



Reaction path II which corresponds to the slow response part



Since both the rates of oxygen adsorption and carbon dioxide desorption are very fast (because the reaction rate is the zero order with respect to P_{O_2} and the transient response of CO₂ shows the instantaneous mode) in the reaction path I, k_I is easily calculated from the graphical analysis of the response curve of CO₂ formed. In reaction path II, k_{II} , $k_{II}CO_2$ and K_{CO_2} are also calculated from the linear plot of P_{CO} / r_{II} vs. P_{CO_2} because r_I can separately be evaluated. All the kinetic parameters obtained are summarized in Table 2.

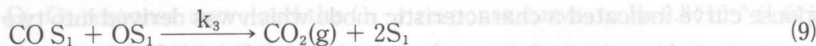
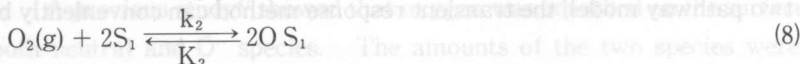
Table 2. Summary of the calculated parameters (Kan-ZnO).

Temp.	$k_I / 10^{-6}$	$k_{II} / 10^{-6}$	$k_{II}CO_2 / 10^{-7}$	K_{CO_2}
190°C	0.26	0.39	0.219	991
200°C	0.50	0.5	0.435	650
225°C	2.1	0.69	2.14	112
250°C	6.6	1.1	9.07	27.5

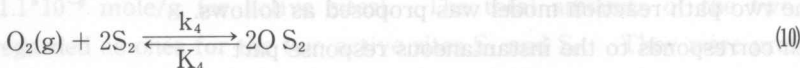
3-4. Reaction Model on K25-ZnO

In our previous paper⁵⁾, it has been demonstrated that the steady state rate has both a maximum and a minimum points, which can not be explained by a single reaction pathway model. The following two reaction pathway model is proposed.

Reaction path I



Reaction path II



All the kinetic parameters are evaluated by the steady state rate analysis using a linear estimation technique as shown in Fig. 4 for P_{O_2} and in Fig. 5 for P_{CO} . The values of kinetic parameters are presented in Table 3.

For reaction path II, k_5 can easily be evaluated from the initial height (Δr_{E-R}) of the instantaneous response curve at P_{CO} higher than $P_{\text{CO}} = 0.40$ atm, in which reaction path II is advantage¹¹⁾. Δr_{E-R} is plotted as a function of the values of CO-concentration jump (ΔP_{CO}) employed in the transient response and it is shown in Fig. 6. From the slope of the straight lines obtained, one can calculate k_5 at all temperatures and they are presented in Table 3.

By using the kinetic parameters obtained, one can visualize a rate surface of total reaction as shown in Fig. 7. As can be seen, the predicted rate surface over the whole range of feed composition reflects the effects of carbon monoxide and oxygen partial pressures on the rate

graphical analysis of the response curve of CO formed. In reaction path II, k_5 can be evaluated separately. k_{CO} are also calculated from the linear plot of P_{CO} vs. P_{CO} because it can be separated.

All the kinetic parameters ($k_1, k_2, k_3, k_4, k_5, K_1, K_2, K_4$) are evaluated.

Table 3. Values of the calculated parameters ($k_1, k_2, k_3, k_4, k_5, K_1, K_2, K_4$) at different temperatures.

Temp. (°C)	k_1	k_2	k_3	k_4	k_5	K_1	K_2	K_4
130	0.01	0.01	0.01	0.01	0.01	0.01	0.01	0.01
140	0.01	0.01	0.01	0.01	0.01	0.01	0.01	0.01
150	0.01	0.01	0.01	0.01	0.01	0.01	0.01	0.01
160	0.01	0.01	0.01	0.01	0.01	0.01	0.01	0.01
170	0.01	0.01	0.01	0.01	0.01	0.01	0.01	0.01

Fig. 4. Linear correlation of the steady state rate data as a function of P_{O_2} on K25-ZnO. The plot shows the rate $(\frac{P_{\text{CO}} P_{\text{O}_2}^{1/2}}{I_{L-H}})^{1/2}$ versus $P_{\text{O}_2}^{1/2}$ (atm) for temperatures 130°C, 140°C, 150°C, 160°C, and 170°C. The data points are fitted with linear regression lines.

Fig. 4. Linear correlation of the steady state rate data as a function of P_{O_2} on K25-ZnO.

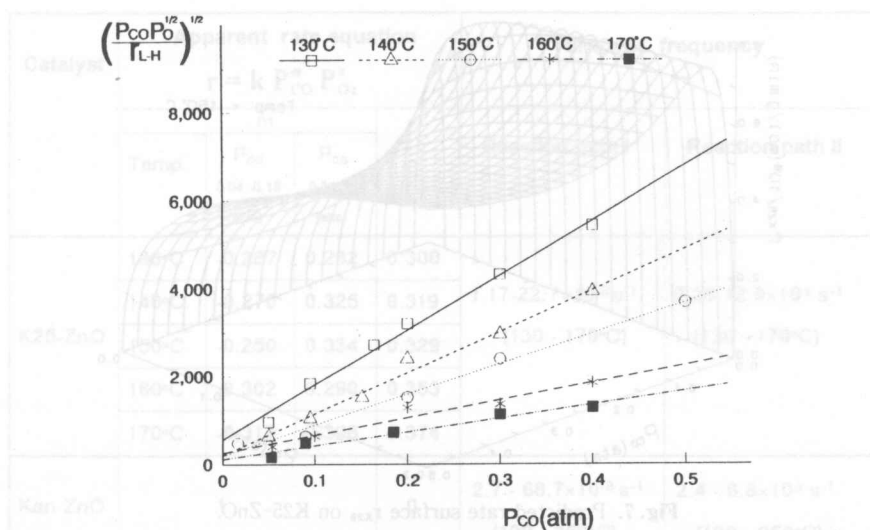


Fig. 5. Linear correlation of the steady state rate data as a function of P_{CO} on K25-ZnO.

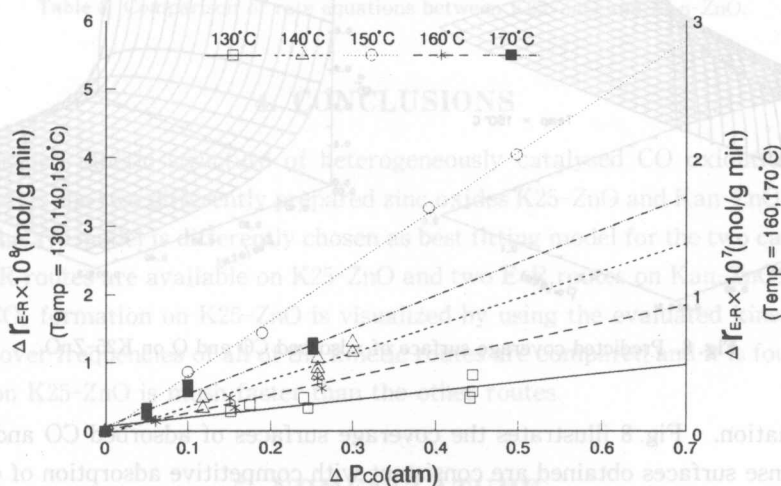


Fig. 6. Plots of Δr_{E-R} vs. ΔP_{CO} on K25-ZnO.

Table 3. Summary of the calculated parameters (K25-ZnO).

Temp.	k_1, k_2	K_1	K_2	k_3	k_4	K_4	k_5
130°C	3.88×10^{-5}	249	382	7.76×10^{-8}	9.25×10^{-6}	105	1.85×10^{-8}
140°C	8.10×10^{-5}	198	208	1.62×10^{-7}	2.63×10^{-5}	30.4	5.26×10^{-8}
150°C	1.73×10^{-4}	145	113	3.46×10^{-7}	6.85×10^{-5}	10.1	1.37×10^{-7}
160°C	4.01×10^{-4}	122	65.1	8.02×10^{-7}	1.63×10^{-4}	3.1	3.25×10^{-7}
170°C	7.50×10^{-4}	103	34.8	1.50×10^{-6}	4.25×10^{-4}	1.14	8.50×10^{-7}

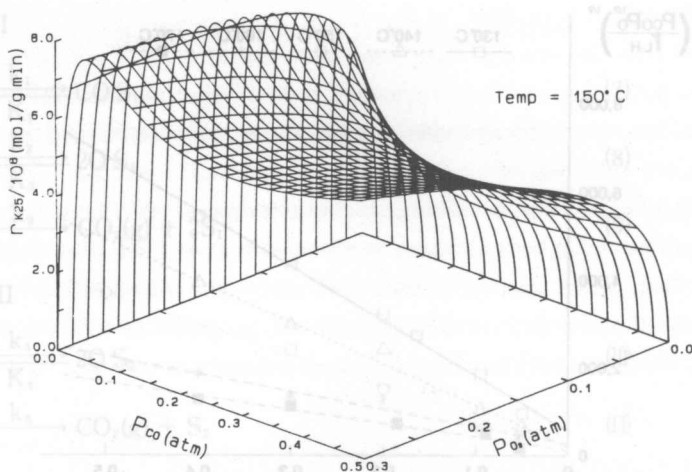


Fig. 7. Predicted rate surface Γ_{K25} on K25-ZnO.

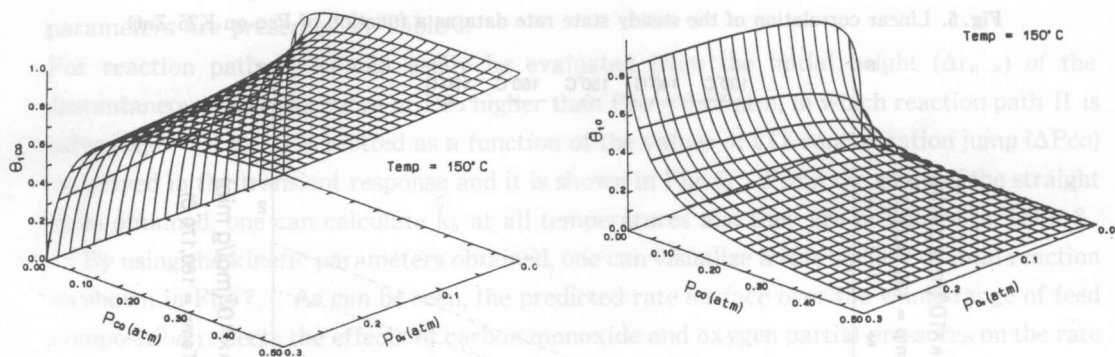


Fig. 8. Predicted coverage surface of adsorbed CO and O on K25-ZnO.

of CO_2 formation. Fig. 8 illustrates the coverage surfaces of adsorbed CO and oxygen. These response surfaces obtained are consistent with competitive adsorption of oxygen and carbon monoxide.

3-5. Surface Reactivity of K25 and Kan-ZnO

The two zinc oxides indicate almost same pattern of X-ray diffraction even though they give a big difference of surface area. Based on the surface area, the turnover frequency (T. F.) of CO_2 formation for the two catalysts can be compared by using an extrapolation at 190°C for K25-ZnO and the values are presented in Table 4. The L-H mechanism in reaction path I on K25-ZnO shows higher value of T.F. ($9.32 \cdot 10^{-2} \text{ s}^{-1}$) than ones of E-R mechanism ($6.24 \cdot 10^{-2} \text{ s}^{-1}$). In reaction path II, T. F. on K25-ZnO ($6.24 \cdot 10^{-2} \text{ s}^{-1}$) is also much higher than one on Kan-ZnO ($2.4 \cdot 10^{-3} \text{ s}^{-1}$). From these results, one may recognize that K25-ZnO has much reactive surface rather than Kan-ZnO. In the present study, one can not clarify the reason why the former is much active. One possible explanation will be considered to be the difference of the form of crystallites, as has been reported by Bolis et al¹⁾.

Catalyst	Apparent rate equation				Turnover frequency	
	$r = k P_{CO}^m P_{O_2}^n$				Reaction path I	Reaction path II
	Temp.	m		n		
P_{CO} 0.04 - 0.18 (atm)		P_{CO} 0.34 - 0.7 (atm)				
K25-ZnO	130°C	-0.287	0.282	0.300	1.17-22.7×10 ⁻³ s ⁻¹ (130 - 170°C)	0.28-12.9×10 ⁻³ s ⁻¹ (130 - 170°C)
	140°C	-0.270	0.325	0.319		
	150°C	-0.250	0.334	0.329		
	160°C	-0.302	0.290	0.353		
	170°C	-0.317	0.336	0.374		
Kan-ZnO		1		0	2.7 - 68.7×10 ⁻³ s ⁻¹ (190 - 250°C)	2.4 - 6.8×10 ⁻³ s ⁻¹ (190 - 250°C)

Table 4. Comparison of rate equations between K25-ZnO and Kan-ZnO.

4. CONCLUSIONS

The detailed kinetic structure of heterogeneously catalysed CO oxidation has been demonstrated on the two differently prepared zinc oxides K25-ZnO and Kan-ZnO. The two reaction pathways model is differently chosen as best fitting model for the two catalysts: the L-H and E-R routes are available on K25-ZnO and two E-R routes on Kan-ZnO. The rate surface of CO₂ formation on K25-ZnO is visualized by using the evaluated kinetic parameters. Turnover frequencies of all of the kinetic routes are compared and it is found that the L-H route on K25-ZnO is much faster than the other routes.

5. NOMENCLATURE

E-R: Eley-Ridel mechanism

K_{CO_2} , K_1 , K_2 , K_4 : equilibrium constant for equations (6), (7), (8) and (10), respectively (atm⁻¹)

k_{II,CO_2} , k_1 , k_2 , k_4 : forward rate constant for equations (6), (7), (8) and (10), respectively (mol/g min atm)

k_I , k_{II} , k_3 : rate constant for equation (1), (4) and (9) (mol/g min)

k_5 : rate constant for equation (11) (mol/g min atm)

L-H: Langmuir-Hinshelwood mechanism

P_{CO} : partial pressure of CO (atm)

P_{O_2} : partial pressure of O₂ (atm)

r_{KAN} , r_{K-25} : steady state rates of CO formation on Kan-ZnO and K25-ZnO, respectively (mol/g min)

Δr_{E-R} : differential reaction rate of E-R part evaluated by the CO-CO response curve (mol/

g min)

S_I, S_{II} : active site for catalytic reaction path I and II, respectively (-)

T : temperature (K)

T. F. : turnover frequency (rate constant at rate determining step/total amount of active site S_I or S_{II}) (s^{-1})

W : weight of catalyst (g)

σ : electrical conductivity of the catalyst ($\Omega^{-1} \text{ cm}^{-1}$).

6. REFERENCES

- 1) Bolis, V., Fubini, B. and Giamello, E. J. Chem. Soc., Faraday Trans. 1, 85, 855 (1989).
- 2) Ohtsuka, K., Tanaka, K. and Tamaru, K., Nippon Kagaku Zasshi, 88, 830 (1987).
- 3) Matsuura, I., Kubokawa, Y. and Toyama, O., Nippon Kagaku Zasshi, 81, 997 (1960).
- 4) Kobayashi, M., Kanno, T. and Kimura, T., J. Chem. Soc. Faraday Trans. 1., 84, 2099 (1988).
- 5) Kobayashi, M., Kobayashi, H. and Kanno, T., Chem. Eng. Comm., 66, 23 (1988).
- 6) Amigues, P. and Teichner, S.J., Discuss. Faraday Soc., 41, 362 (1966).
- 7) Yoshitake, H. and Iwasawa, Y., J. Catal. 125, 227 (1990).
- 8) Kobayashi, H. and Kobayashi, M., Catal. Rev. Eng. Sci., 10, 104 (1974).
- 9) Bennet, C. O., Catal. Rev. Eng. Sci., 12, 105 (1976).
- 10) Kobayashi, M. and Kobayashi, H. J. Catal. 27, 180 (1972).
- 11) Hakozaki, M., Golman B., Kanno T. and Kobayashi M., Memoirs of KIT, 24, 17 (1992).